Article:

Lu, H, Zhang, A, Yao, Y et al. (1 more author) (2016) Phenomenological model and working mechanism of bio-inspired polymeric composites driven by water gradient. Pigment and Resin Technology, 45 (1). pp. 62-70. ISSN 0369-9420

https://doi.org/10.1108/PRT-04-2015-0040

Phenomenological model and working mechanism of bio-inspired polymeric composites driven by water gradient

Abstract

Purpose – To develop a phenomenological model to investigate the underlying mechanism of and to predict the bio-inspired performance under different thermo-temporal conditions.

Design/methodology/approach – Flory-Rehner free-energy functions are applied to quantitatively identify the driving forces in the viscously bio-inspired response of dynamic polymer network. Furthermore, permeation transition equation is adopted to couple water gradient and water sorption/desorption into the free-energy function.

Findings – The results show that the influence of potential energy on deformation can be related to a stretching ratio that uniquely determines water sorption/desorption, locomotion frequency and contractile stress. Finally, by means of combining the free-energy function and Arrhenius equation, a phenomenological thermo-temporal model is developed and verified by the experimental results.

Research implications – This study focuses on exploring the theoretical mechanism and significantly enhances understanding of relevant experimental features reported previously.

Originality/value – The outcome of this study will provide a powerful phenomenological and quantitative tool for study of shape memory effect in bio-inspired polymers.

Keywords - Bio-inspired polymer, Free-energy function, Thermo-temporal, Phenomenological modelling

Paper type Research paper

Introduction

Bio-inspired polymers are a class of responsive materials that are able to derive their phenomenal properties from precisely controlled sequences and compositions of the constituents, which in turn lead to rearrangement of chain shapes and structures on external stimuli (Yu and Cölfen, 2004; Xia and Jiang, 2008; Venkatraman *et al*., 2008). Bio-inspired polymers can adapt to surrounding environment and convert chemical or biochemical signals into thermal, optical, electrical and mechanical signals, and vice versa (Jones *et al*., 1991; Bao and Suresh, 2003; Ayari *et al*., 2007; Stuart *et al*., 2010; Lu and Huang, 2013). The stimuli-responsive macromolecules are capable of conformational and chemical changes on receiving an external signal, accompanied by variations in the physical properties and thermo-temporal conditions of the polymer and derived from changes in the materials' environment (Gitsov and Fréchet, 1996; Liu and Urban, 2010; Roy *et al*., 2010; Mather *et al*., 2009). To intelligently design such systems, the novel physics and working mechanism of the bio-inspired polymers have been focused on in previous works (Börner, 2007; Creton and Gorb, 2007). Many effective approaches are aimed to apply biological components or biological design principles to dramatically extend their capability and applicability (Kim *et al*., 2005; Trask *et al*., 2007; Zhang *et al*., 2012; Cianchetti *et al*., 2009). Currently, these bio-inspired materials are playing an increasingly important role in a diverse range of applications, particularly in biomedical field (e.g. scaffolds for tissue engineering) (Pham *et al*., 2006), pharmaceutical science (e.g., drug delivery devices) (Flores *et al*., 2013), environmental science (Hu *et al*., 2012), and nanotechnology (Ding *et al*., 2007).

To enable biological functions, nature requires to selectively tailor molecular assemblies that provide a specific chemical function and structure (O'Reilly *et al*., 2006). Bio-inspired and synthetic polymer composites are often prepared and actuated via mimicking the action of muscles that are capable of responding to the environment (Smela, 2003; Ebron *et al*., 2006). A bio-inspired material, which is to absorb water and change its shape, has been designed by combining both a stiff polypyrrole (PPy) and a dynamic polyolborate network that is hydrolytically sensitive could be driven by water gradient (Ma *et al*., 2013). The polyolborate network is sensitive to water by means of hydrolysis and reform of the borate ester crosslinking hub upon water sorption and desorption, and thus changes the mechanical properties of the composite (Ma *et al.*, 2013). The polymer composite could exchange water with the environment to induce expansion or contraction (Ma *et al.*, 2013). The mechanical energy converted from the chemical potential energy of bio-inspired polymeric composites has been identified as the driving force (Lu and Huang, 2013; Lu *et al.*, 2014). In this study, Flory-Rehner free-energy functions are employed to quantitatively separate the effect and identify the driving force in bio-inspired viscous response of dynamic polymeric network. Working mechanism and bio-inspired performance under different thermo-temporal conditions have been investigated and modelled. By means of combining free-energy function and Arrhenius equation together, the influence of potential energy on deformation can be related by a stretching ratio that uniquely determines water sorption/desorption, locomotion frequency and contractile stress of this water gradient-driven polymeric composite. The phenomenological thermo-temporal model is verified by the available experimental results in the literature. This study focuses on the theoretical mechanism, which is a challenging issue and will significantly enhance our understanding of these experimental features.

The theoretical framework

Flory-Rehner free energy equation is generally employed to describe thermodynamic of polymer solution, by comparing the free energy function before and after mixing (Lu, 2012). For the given bio-inspired PEE-PPy composite, water molecules penetrate into the polymer network and mix with the polyolborate macromolecules. There are two contributions to the free-energy function (W) of the bio-inspired dynamic polymeric composite driven by water gradient in a water sorption and desorption cycle: stretching free-energy (W_s) and mixing free-energy (W_m) (Du and Zhang, 2010; Lu e*t al.*, 2010), i.e.

$$W = W_s + W_m \tag{1}$$

The free-energy of stretching a network denotes the stretches ($\lambda_1, \lambda_2, \lambda_3$) of the polymer by (He and Chen, 2000)

$$W_s(\lambda_1, \lambda_2, \lambda_3) = \frac{1}{2} NkT(\lambda_1{}^2 + \lambda_2{}^2 + \lambda_3{}^2 - 3 - 2\log \lambda_1\lambda_2\lambda_3) \tag{2}$$

where N is the number of chains in the polymer divided by the volume of the polymer block in the referenced state, and kT is the energy of the individual particle in certain temperature.

Without the cross-linking network, polymer can be dissolved and form a solution. As the PEE-PPy composite driven by water gradient, the dynamic polyolborate network is hydrolytically sensitive to water by means of hydrolysis and reforming of the borate ester crosslinking hub upon water sorption and desorption. Here the mixing free-energy is taken as (He and Chen, 2000),

$$W_m(C) = \frac{kT}{\nu}\left[\nu C \log\left(1+\frac{1}{\nu C}\right)+\frac{\chi}{1+\nu C}\right] \tag{3}$$

where C is the number of the solvent molecules in the polymeric network and v is the volume of per solvent molecule. νC is the volume of the solvent molecules in the network divided by the volume of the polymers. Thus, Equation 3 can be substantiated by,

$$W = \frac{1}{2}NkT(\lambda_1^2+\lambda_2^2+\lambda_3^2-3-2\log\lambda_1\lambda_2\lambda_3)+\frac{kT}{\nu}\left[\nu C\log\left(1+\frac{1}{\nu C}\right)+\frac{\chi}{\left(1+\nu C\right)}\right] \tag{4}$$

Considering a cubic solvent-swollen polymer without constraint to be stretched in three directions, and the stretches of polymer to a fixed value, namely $\lambda_1, \lambda_2, \lambda_3$. In the referenced state, no external loadings are applied on the block, and no solvent molecules are absorbed inside the block with dimensions of $L_1 L_2 L_3$. Exposing the polymer to solvent, the polymeric block is assumed to imbibe solvent molecules that diffuse into the interstitial space of the polymer chains. It is assumed that weights applied on the six surfaces of the block results in the dimensions of polymeric block changed to $l_1 l_2 l_3$ (Zhao and Suo, 2007). Denote the stretches of the block by,

$$\lambda_1 = \frac{l_1}{L_1},\ \lambda_2 = \frac{l_2}{L_2},\ \lambda_3 = \frac{l_3}{L_3}. \tag{5}$$

It is assumed that both polymer molecules and solvent molecules are incompressible, as well as there is no void space inside the polymer block. When C solvent molecules are diffused into polymer, the volume of the polymer changes to $\lambda_1\lambda_2\lambda_3 = 1+\nu C$.

Considering a cubic solvent-swollen polymer without constraint to be stretched in three directions, and the stretches of polymer to a fixed value, namely $\lambda_1 = \lambda_2 = \lambda_3 = \lambda$. Thus the ($1 + \nu C$) can be calculated by substituting λ into Equation 3, namely, $1 + \nu C = \lambda^3$. Equation 4 can be rewritten as,

$$\frac{vW}{kT} = \frac{3}{2} Nv(\lambda^2 - 1 - 2\log\lambda) + \left[(\lambda^3 - 1)\log\left(\frac{\lambda^3}{\lambda^3 - 1}\right) + \frac{\chi}{\lambda^3} \right] \quad (6)$$

where Nv is assumed to be a constant. Meanwhile when a cubic polymer is subject to a uniaxial stress along the longitudinal direction, it is under the uniaxial stress. The state of deformation can be characterized by the longitudinal stretch λ_1 and two transverse stretches $\lambda_2 = \lambda_3$. In this case, $1 + vC = \lambda_1 \lambda_2^2$, the Equation 6 may be expressed as,

$$\frac{vW}{kT} = \frac{1}{2} Nv(\lambda_1^2 + 2\lambda_2^2 - 3 - 2\log\lambda_1\lambda_2^2) + \left[\left(\lambda_1\lambda_2^2 - 1\right)\log\left(\frac{\lambda_1\lambda_2^2}{\lambda_1\lambda_2^2 - 1}\right) + \frac{\chi}{\lambda_1\lambda_2^2} \right] \quad (7)$$

Figures 1(a) and (b) plots numerical results for free energy function with stretching ratio of PEE-PPy composite in mixing with water, where $N\nu$ is assumed to be a constant. As presented in Equation 7, the change in free energy function is determined by two parameters, namely χ and λ_2/λ_1, while it is essentially determined by the free-energy of stretching or free-energy of mixing in a certain range of stretching ratio.

(Take in Figure 1)

When PEE-PPy composite is immersed into water, water molecules are penetrated into the polymer network. Transport and immigration of water molecules is originated from the permeability (P) of PEE-PPy composite. In such a case, it is a common practice to characterize mass transfer by the permeation flux (Roy, 1999; Ashley, 1985),

$$J = \frac{\phi_2 \cdot d}{A \cdot t} \quad (8)$$

where J is the normalized flux, ϕ_2 is the amount of water molecule, d is the thickness of polymer, A is the surface area of polymer, and t is the permeation time. Equation (8) may be rewritten as (Roy, 1999; Ashley, 1985),

$$\phi_2 = P\frac{A \cdot t \cdot p}{d} \quad \left(J = P \cdot p\right) \tag{9}$$

where p is osmotic pressure applied upon the polymer. We assume that individual PEE-PPy macromolecule and the mobile water molecule are incompressible. Assume that one unit of the dry macromolecules imbibes C numbers of water molecules and swells to $\lambda_1, \lambda_2, \lambda_3$. The water molecules contribute to the swelling of the polymer, the volume fraction of water molecules in PPy/water system is therefore presented as,

$$\phi_2 = \frac{\nu C}{1+\nu C} = \frac{\lambda_1\lambda_2\lambda_3 - 1}{\lambda_1\lambda_2\lambda_3} \tag{10}$$

In combination of Equations 9 and 10, the constitutive relation between the pressure and stretch may be expressed as,

$$P\frac{A \cdot t \cdot \sigma}{d} = \frac{\lambda_1\lambda_2\lambda_3 - 1}{\lambda_1\lambda_2\lambda_3} \tag{11}$$

As the polymer area A and thickness d can be written as $A = \lambda_1\lambda_2$ and $d = \lambda_3$, respectively, Equation 11 may be rewritten as,

$$\phi_2 = P\frac{\lambda_1 \cdot \lambda_2 \cdot t \cdot \sigma}{\lambda_3} \xrightarrow{\lambda_2 = \lambda_3} \phi_2 = P\left(\lambda_1 \cdot t \cdot \sigma\right) = \frac{\lambda_1\lambda_2^2 - 1}{\lambda_1\lambda_2^2} \Rightarrow \sigma = \frac{\lambda_1\lambda_2^2 - 1}{P\left(\lambda_1^2\lambda_2^2 \cdot t\right)} \tag{12}$$

Figure 2 plots the constitutive relation of stress and stretching ratio. The numerical results reveal the trend as expected, i.e., with the increase of stretching ratio of (λ_2/λ_1), higher pre-stress is needed, resulting in the decreasing of stress which is originated from osmotic pressure. On the other hand, the stress initially increases and then decreases with the increase in the stretching ratio of PEE-PPy composite where $\lambda_2/\lambda_1 = 1$, $\lambda_2/\lambda_1 = 1.25$ and $\lambda_2/\lambda_1 = 1.5$. The stress initially increases with the increase in the stretching ratio due to the change in the area of polymer. And then it gradually decreases because the volume fraction of water molecules and pre-stress increase significantly.

(Take in Figure 2)

Constitutive relationship and phenomenological modelling

Constitutive modelling of stretching ratio and frequency

The PEE-PPy composite continuously flips and navigates due to water gradient, resulting from the nonuniform water absorption and asymmetric swelling of the bottom and top faces. Therefore, water gradient is reflected in the asymmetric film deformation and drives the polymer composite locomotion (Ma *et al.*, 2013). Assume that a unit volume of dry PEE-PPy composite imbibes C numbers of water molecules and swells to a volume of $1+\nu C=\lambda^3$ as the constituents are assumed to be a kind of incompressible. By the combination of Equations 11 and 12, the relationship between volume concentration of water and stretching ratio in a homogeneous state of deformation for free swelling (where $\lambda_1=\lambda_2=\lambda_3=\lambda$) can be obtained as,

$$\phi=\frac{\nu C}{1+\nu C}=\frac{\lambda^3-1}{\lambda^3}\rightarrow\lambda=\left(\frac{1}{1-\phi}\right)^{1/3}=\left(\frac{1}{1-P\cdot\dfrac{S\cdot t\cdot p}{d}}\right)^{1/3}\qquad(13)$$

where permeability of water solvent is of 10^{-8} $cm^2\cdot s^{-1}\cdot Pa^{-1}$, polymer area S is 1.7 cm×3 cm and the thickness d is 3×10^{-2} cm (He and Chen, 2000). Here Equation 13 can be expressed as,

$$\lambda=\left(\frac{1}{1-t\cdot p\cdot1.7\times10^{-6}}\right)^{1/3}\qquad(14)$$

Figures 3(a) and (b) plot the numerical results of stretching ratio as a function of the immersion time and saturated water vapour pressure of polymer, respectively. The change in the stretching ratio of PEE-PPy composite may affect the quantitative results and maintain the overall trend. Simulation shows the expected trend, i.e., the stretching ratio increases with an increase in immersion time and saturated water vapour pressure. As the immersion time and saturated water vapour pressure gradually increases, many more incompressible water molecules are absorbed into the polymer composite, resulting in the volume of polymer mixture and stretching ratio increased.

(Take in Figure 3)

Polymer material obeys the relaxation rule, and the relationship between relaxation time and internal activation energy follows Eyring equation as (Nguyen1 *et al*., 2010; Li and Xu, 2011; Lu, 2013),

$$\frac{1}{f}=\frac{1}{f_0}\exp(\frac{\Delta E}{RT}) \tag{15}$$

where f is the relaxation frequency, ΔE is the internal activation energy of chain mobility, R is the gas constant, T is the absolute temperature and f_0 is a given constant. As well known, the bio-inspired PEE-PPy composite is of elastic shape change in the mechanical cycle of shape change. The change in free energy is assumed to be equal to the internal activation energy that is the driving force for the water-gradient-induced shape change. Then, the Equation 15 can be rewritten as,

$$\frac{1}{f}=\frac{1}{f_0}\exp(\frac{W}{kT}) \tag{16}$$

In combination of Equations 6 and 16, the frequency can be expressed,

$$\frac{1}{f}=\frac{1}{f_0}\exp\left(\frac{1}{\nu}\right)\cdot\left\{\frac{3}{2}N\nu(\lambda^2-1-2\log\lambda)+\left[(\lambda^3-1)\log\left(\frac{\lambda^3}{\lambda^3-1}\right)+\frac{\chi}{\lambda^3}\right]\right\} \tag{17}$$

Here, Equations 14 and 17 may be employed to characterise the effect of stretching ratio and saturated water vapour pressure on the frequency of the bio-inspired PEE-PPy composite.

$$\begin{cases}\frac{1}{f}=\frac{1}{f_0}\exp\left(\frac{1}{\nu}\right)\cdot\left\{\frac{3}{2}N\nu(\lambda^2-1-2\log\lambda)+\left[(\lambda^3-1)\log\left(\frac{\lambda^3}{\lambda^3-1}\right)+\frac{\chi}{\lambda^3}\right]\right\} \\ \lambda=\left(\frac{1}{1-t\cdot p\cdot 1.7\times10^{-6}}\right)^{1/3}\end{cases} \tag{18}$$

Figures 4(a) and (b) plot numerical results for frequency with stretching ratio and osmotic pressure, respectively, at a different value of χ and normalized immersion time of t. With an increase in both stretching ratio and osmotic pressure, the frequency of polymer composite gradually decreases in the whole trend. As indicated by Equation (18), the decrease in frequency is only contributed to the increase in the stretching ratio, namely the increase in osmotic pressure also results in the increase of stretching ratio. When the stretching ratio increases, the internal activation energy and free energy are increased, resulted in the frequency decreased according to the Arrhenius law (Lu, 2013).

(Take in Figure 4)

Constitutive modelling of stress and stretching ratio in subject to mechanical loads

A cubic bio-inspired PEE-PPy composite is immersed in water. It is assumed that polymer composite imbibes water molecules, resulting in its volume expansion. Thermodynamics dictates that the free-energy reaches minimum as the polymer/water system becomes stable. Here, the stresses may be expressed as (Zhao and Suo, 2007),

$$S_1 = \frac{\partial W}{\partial \lambda_1},\ \ S_2 = \frac{\partial W}{\partial \lambda_2},\ \ S_3 = \frac{\partial W}{\partial \lambda_3} \tag{19}$$

In deriving Equation 19, we have regarded S_1, S_2, S_3 as the loading parameters in three directions of the cubic polymer/water system. It is considered that the length of the cubic PEE-PPy composite is fixed, while two lateral directions are free to move. Let λ_1 be the fixed stretch in the longitude direction by pre-stretching, and λ_2, λ_3 ($\lambda_2 = \lambda_3$) be the stretch in other directions, thus, $1 + vC = \lambda_1 \lambda_2^2$. Here, in a constraint state the constitutive relationship between stress and stretching ratio can be expressed as,

$$\frac{vS_1}{kT} = \frac{v}{kT}\frac{\delta W}{\delta \lambda_1} = 3\lambda_2^2 \log\left(1 - \frac{1}{\lambda_1 \lambda_2^2}\right) + \frac{3}{\lambda_1} + \frac{3\chi}{\lambda_1^2 \lambda_2^2} + Nv\left[\lambda_1\left(1 + \frac{2\lambda_2^2}{\lambda_1^2}\right) - \frac{3}{\lambda_1}\right] \tag{20}$$

Equation 20 gives the equilibrium of vs_1/kT function for the water gradient-induced PEE-PPy composite subjected to a longitudinal loading. The characteristic of vS_1/kT, using

χ and stretch ratio λ_1/λ_2 as parameters is plotted in Figure 5. Figures 5(a) and (b) plot the relationship between vs_1/kT function and stretch ratio λ_1/λ_2. For a given parameter, e.g. $\chi = 0$, $\chi = 0.5$, $\chi = 0.7$, $\chi = 1.0$ and $\chi = 1.2$, the vS_1/kT function sharply increases with the increase in stretching ratio in the initial stage. On the other hand, with stretching ratio further increasing, vS_1/kT function decreases more slowly. This numerical result reveals that the stress reaches to a constant value with higher stretch λ_1. And the decrease in vS_1/kT is slower. With the χ increased, the mixing between polymer macromolecules and water molecules becomes difficult, because the free energy function and internal activation energy significantly increase. Here, the stress function therefore increases at the same stretching ratio, as shown in Figure 5(a). Meanwhile, the free energy function also increases with the swelling ratio of polymer, leading to a high value of stress at the same stretching ratio as presented in Figure 5(b). Both numerical results are due to the increase in the free energy function of polymer/water mixed system.

(Take in Figure 5)

Although the above simulation results are used for the constitutive relationship between stress and stretching ratio, it should be noted that each tested sample always presents a different and partial constitutive behaviour due to the difference in the free energy function and internal activation energy. Therefore, Figure 6 is presented and the curves are picked out from Figure 5 for comparison between analytical results and experimental results. Figure 6 presents the numerical results of stress as a function of expansion/contraction cycle times. These analytical results verify that the constitutive relationship between stress and expansion/contraction cycle times in bio-inspired PEE-PPy composite in response to water gradient. We can utilize these to account for the effects of expansion/contraction behaviour on the bio-inspired PEE-PPy composite.

(Take in Figure 6)

Phenomenological modelling of bio-inspired polymer driven by water gradients

As known, the thermodynamics of polymers obey the relaxation rule (Nguyen1 *et al.*, 2010; Li and Xu, 2011; Lu, 2013), which could be employed to theoretically predict the relationships between flipping frequency with the saturated water vapour pressure and transport cargo. Relaxation time of polymers verifies the Arrhenius law: $\tau = \tau_0 \exp\left(\Delta E/RT\right)$. The frequency f fulfils the condition $2\pi f \tau = 1$, which leads to $f_o/f = \exp\left(\Delta E/RT\right)$. According to the theory on the effect of atmospheric pressure and stress on the relaxation behaviour of polymers, the Arrhenius law is modified to $f_o/f = \exp\left[\left(\Delta E - a\sigma\right)/RT\right]$, as the polymer is constrained by atmospheric pressure (p), and V is the volume change. The applicability of this equation can be verified where the increase in the atmospheric pressure (p) is equivalent to the decrease of (f_o/f), therefore increasing the flipping frequency (f) as the activation energy (ΔE) and temperature (T) are kept constant. Here $f_o/f = \exp\left[\left(\Delta E - a\sigma\right)/RT\right]$ can be expressed as,

$$f_o/f = \exp\left[\left(\Delta E - pV\right)/RT\right] \tag{21}$$

It can be found that the frequency gradually increases with the increase in atmospheric pressure (p). The frequency of flipping motion as a function of the saturated water vapour pressure at each substrate temperature indicates an exponential correlation, not a linear correlation. Moreover, an exponential expression is employed to fitting the experimental data, as shown in the Figure 7. Therefore, we substantiate that the frequency of flipping motion and the saturated water vapour pressure indicate an exponential correlation, based on the Arrhenius law and simulation result, respectively.

(Take in Figure 7)

The flipping frequency verifies the Arrhenius law $f_o/f = \exp\left(\Delta E/RT\right)$, the increase in the frequency (f) is equivalent to the decrease in the activation energy (ΔE). And the decrease in the activation energy is equivalent to the decrease in the transport cargo (σ) as the strain (ε) is constant and $\Delta E = \sigma \cdot \varepsilon$. Therefore, the flipping frequency verifies the modified Arrhenius law,

$$f_o / f = \exp\left[(\sigma \cdot \varepsilon)/RT\right] \tag{22}$$

The applicability of this equation can be verified where the decrease in the flipping frequency (f) is equivalent to the increase in the function of $\exp\left[(\sigma \cdot \varepsilon)/RT\right]$, therefore increasing the transport cargo, as the strain (ε) and temperature (T) being kept constant. Figures 8(a) and (b) present the numerical simulation for the effects of pV and $\sigma\varepsilon$ on the flipping frequency of PEE-PPy composite as a function of atmospheric pressure. Furthermore, an exponential equation is employed to verify the accuracy of the Arrhenius law for predicting the correlation of flipping frequency and cargo, as shown in the Figure 9. Based on the fitting curve, it is proven that the applicability of the exponential equation for fitting the experimental data. Here we also substantiate that the flipping frequency and the cargo indicate an exponential correlation, based on the Arrhenius law and simulation result, respectively.

(Take in Figure 8)

(Take in Figure 9)

Concluding remarks

In this study, we validated the effectiveness of a theoretical approach and phenomenological modelling for the underlying mechanism and bio-inspired performance of the PEE-PPy composite driven by water gradient under different thermo-temporal conditions. In this approach, the theoretical and phenomenological models from Flory-Rehner free-energy functions and permeation transition equation provide an effective way to describe and predict the bio-inspired response of PEE-PPy composite. Furthermore, the thermo-temporal and constitutive relationships among locomotion frequency, atmospheric pressure and contractile stress and stretching ratio have been modelled and simulated by means of combining the free-energy function and Arrhenius equation. We verified the accuracy of the analytical results by the available experimental results. In this work, the theoretical approach is developed to identify the working mechanism, characterize the bio-inspired performance and accurately predict bio-inspired behaviour of the PEE-PPy composite driven by water gradients.

References

Ashley, R.J. (1985), “Permeability and plastics packaging, in Polymer permeability”, Netherlands: Springer.

Ayari, A., Vincent, P., Perisanu, S., Choueib, M., Gouttenoire, V., Bechelany, M., Cornu, D. and Purcell, S.T. (2007), “Self-oscillations in field emission nanowire mechanical resonators: A nanometric dc−ac conversion”, *Nano Lett.*, Vol. 7, pp. 2252-7.

Bao, G. and Suresh, S. (2003), “Cell and molecular mechanics of biological materials”, *Nature Mater.,* Vol. 2, pp. 715-25.

Börner, H.G., (2007), “Functional polymer-bioconjugates as molecular LEGO® bricks”, *Macromol. Chem. Phys.*, Vol. 208, pp. 124-30.

Cianchetti, M., Mattoli, V., Mazzolai, B., Laschi, P.D. (2009), “A new design methodology of electrostrictive actuators for bio-inspired robotics”, *Sensor. Actuat. B-Chem.*, Vol. 142, pp. 288-97.

Creton, C. and Gorb, S. (2007), “Sticky feet: from animals to materials”, *MRS Bull.*, Vol. 32, pp. 466-72.

Ding, L., Hao, C., Xue, Y.D. and Ju, H.X. (2007), “A bio-inspired support of gold nanoparticles−chitosan nanocomposites gel for immobilization and electrochemical study of K562 Leukemia cells”, *Biomacromolecules*, Vol. 8, pp. 1341-6.

Du, H.Y. and Zhang, J.H. (2010), “Solvent induced shape recovery of shape memory polymer based on chemically cross-linked poly(vinyl alcohol)”, *Soft Matter*, Vol. 6, pp. 3370-6.

Ebron, R.V.H., Yang, Z.W., Seyer, D.J., Kozlov, M.E., Oh, J.Y., Xie, H., Razal, J., Hall, L.J., Ferraris, J.P., MacDiarmid, A.G. and Baughman, R.H. (2006), “Fuel-powered artificial muscles”, *Science*, Vol. 311, pp. 1580-3.

Flores, E.I.S., Friswell, M.I. and Xia, Y. (2013), “Variable stiffness biological and bio-inspired materials”, *J. Intel. Mat. Syst. Str.*, Vol. 24, pp. 529-40.

Gitsov, I. and Fréchet, J.M.J. (1996), "Stimuli-responsive hybrid macromolecules: novel amphiphilic star copolymers with dendritic groups at the periphery", *J. Am. Chem. Soc.*, Vol. 118, pp. 3785-6.

He, M.J. and Chen, W.X. (2000), *Polymer Physics*, Fudan University Press.

Hu, J.L., Zhu, Y., Huang, H.H. and Lu, J. (2012), "Recent advances in shape-memory polymers: Structure, mechanism, functionality, modelling and applications", *Prog. Polym. Sci*., Vol. 37, pp. 1720-63.

Jones, D.B., Nolte, H., Scholübbers, J.G., Turner, E. and Veltel, D. (1991), "Biochemical signal transduction of mechanical strain in osteoblast-like cells", *Biomaterials*, Vol. 12, pp. 101-10.

Kim, S.J., Kim, H.Il., Park, S.J., Kim, I.Y., Lee, S.H., Lee, T.S. and Kim, S.I. (2005), "Behavior in electric fields of smart hydrogels with potential application as bio-inspired actuators", *Smart Mater. Struct*., Vol. 14, pp. 511-4.

Liu, F. and Urban, M.W. (2010), "Recent advances and challenges in designing stimuli-responsive polymers", *Prog. Polym. Sci.*, Vol. 35, pp. 3-23.

Li, G.Q. and Xu, W. (2011), "Thermomechanical behaviour of thermoset shape memory polymer programmed by cold-compression: Testing and constitutive modelling", *J. Mech. Phys. Solids*., Vol. 59, pp. 1231-50.

Lu, H.B. (2012), "A simulation method to analyze chemo-mechanical behaviour of swelling-induced shape-memory polymer in response to solvent", *J. Appl. Polym. Sci.*, Vol. 123, pp. 1137-46.

Lu, H.B. (2013), "Comment on "Mechanisms of the multi-shape memory effect and temperature memory effect in shape memory polymers" by L. Sun and W. M. Huang, Soft Matter, 2010, 6, 4403", *Soft Matter*, Vol. 9, pp. 11157-8.

Lu, H.B. and Huang, W.M. (2013), "A phenomenological model for the chemoresponsive shape memory effect in amorphous polymers undergoing viscoelastic transition", *Smart Mater. Struct*., Vol. 22, pp. 115020.

Lu, H.B. and Huang, W.M. (2013), "On the origin of Vogel-Fulcher-Tammann Law in the thermo-responsive shape memory effect of amorphous polymers", *Smart Mater. Struct.*, Vol. 22, pp. 105021.

Lu, H.B., Huang, W.M. and Leng, J.S. (2014), "A phenomenological model for simulating the chemo-responsive shape memory effect in polymers undergoing a permeation transition", *Smart Mater. Struct.*, Vol. 23, pp. 045038.

Lu, H.B., Liu, Y.J., Leng, J.S. and Du, S.Y. (2010), "Qualitative separation of the physical swelling effect on the recovery behaviour of shape memory polymer", *Eur. Polym. J.*, Vol. 46, pp. 1908-14.

Ma, M.M., Guo, L., Anderson, D.G. and Langer, R. (2013), "Bio-inspired polymer composite actuator and generator driven by water gradients", S*cience*, Vol. 339, pp. 186-9.

Mather, P.T., Luo, X.F. and Rousseau, I.A. (2009), "Shape memory polymer research Annu.", *Rev. Mater. Res.*, Vol. 39, pp. 445–71.

Nguyen1, T.D., Yakacki, C.M., Brahmbhatt, P.D. and Chambers, M.L. (2010), "Modelling the Relaxation Mechanisms of Amorphous Shape Memory Polymers", *Adv. Mater.*, Vol. 22, pp. 3411-23.

O'Reilly, R.K., Hawker, C.J. and Wooley, K.L. (2006), "Cross-linked block copolymer micelles: functional nanostructures of great potential and versatility", *Chem. Soc. Rev.*, Vol. 35, pp. 1068-83.

Pham, Q.P., Sharma, U. and Mikos, A.G. (2006), "Electrospinning of polymeric nanofibers for tissue engineering applications: A review", *Tissue Eng.*, Vol. 12, pp. 1197-211.

Roy, D., Cambre, J.N and Sumerlin, B.S. (2010), "Future perspectives and recent advances in stimuli-responsive materials", *Prog. Polym. Sci.*, Vol. 35, pp. 278-301.

Roy, S. (1999), "Modelling of anomalous moisture diffusion in polymer composites: A finite element approach", *J. Compos. Mater.*, Vol. 33, pp. 1318-43.

Smela, E. (2003), "Conjugated polymer actuators for biomedical applications", *Adv. Mater.*, Vol. 15, pp. 481-94.

Stuart, M.A., Huck, W.T.S., Genzer, J., Müller, M., Ober, C., Stamm, M., Sukhorukov, G.B., Szleifer, I., Tsukruk, V.V., Urban, M., Winnik, F., Zauscher, S., Luzinov, I. and Minko, S. (2010), "Emerging applications of stimuli-responsive polymer materials", *Nature Mater.*, Vol. 9, pp. 101-13.

Trask, R.S., Williams, H.R. and Bond, I.P. (2007), "Self-healing polymer composites: mimicking nature to enhance performance", *Bioinspir. Biomim.*, Vol. 2, pp. 1-9.

Venkatraman, S., Boey, F. and Lao, L.L. (2008), "Implanted cardiovascular polymers: Natural, synthetic and bio-inspired", *Prog. Polym. Sci.*, Vol. 33, pp. 853-74.

Xia, F. and Jiang, L. (2008), "Bio-inspired, smart, multiscale interfacial materials", *Adv. Mater.*, Vol. 20, pp. 2842-58.

Yu, S.H. and Cölfen, H. (2004), "Bio-inspired crystal morphogenesis by hydrophilic polymers", *J. Mater. Chem.*, Vol. 14, pp. 2124-47.

Zhang, L., Wu, J., Wang, Y., Long, Y., Zhao, N. and Xu, J. (2012), "Combination of bioinspiration: A general route to superhydrophobic particles", *J. Am. Chem. Soc.*, Vol. 134, pp. 9879-81.

Zhao, X. and Suo, Z. (2007), "Method to analyze electromechanical stability of dielectric elastomers" *Appl. Phys. Lett.*, Vol. 91, pp. 061921.

Figure 1 Numerical simulation of the constitutive relation of free energy function and stretching ratio. (a) χ =0.0, 0.2, 0.5, 0.7, 1.0 and 1.2; (b) λ_2/λ_1 =1.0, 1.5, 2.0, 2.5 and 3.0.

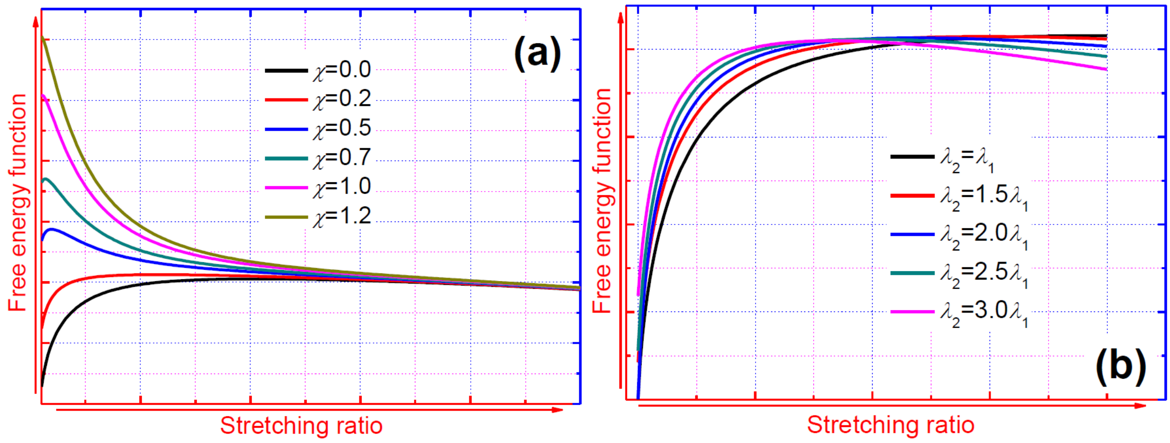

Figure 2 Numerical simulation for the constitutive relation of stress and stretch

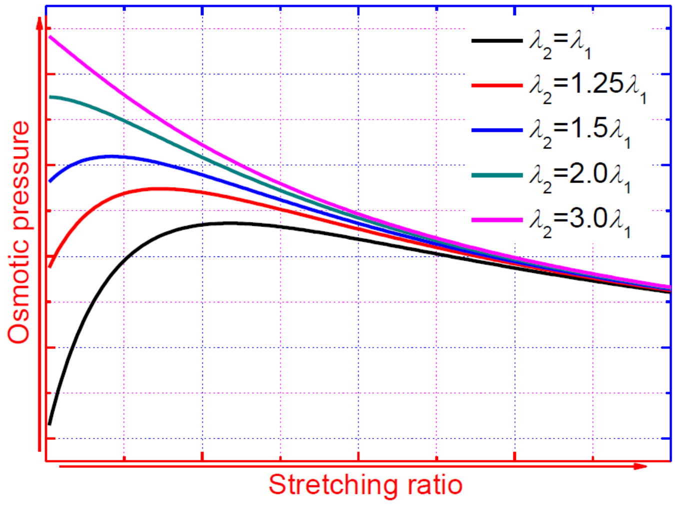

Figure 3 Numerical simulation for the effect of immersion time and saturated water vapour pressure on the stretching ratio of PPy/water system. (a) Saturated water vapour pressure is of 10, 20, 30, 40 and 50 kPa; (b) Normalised time is of 2, 4, 6, 8 and 10t.

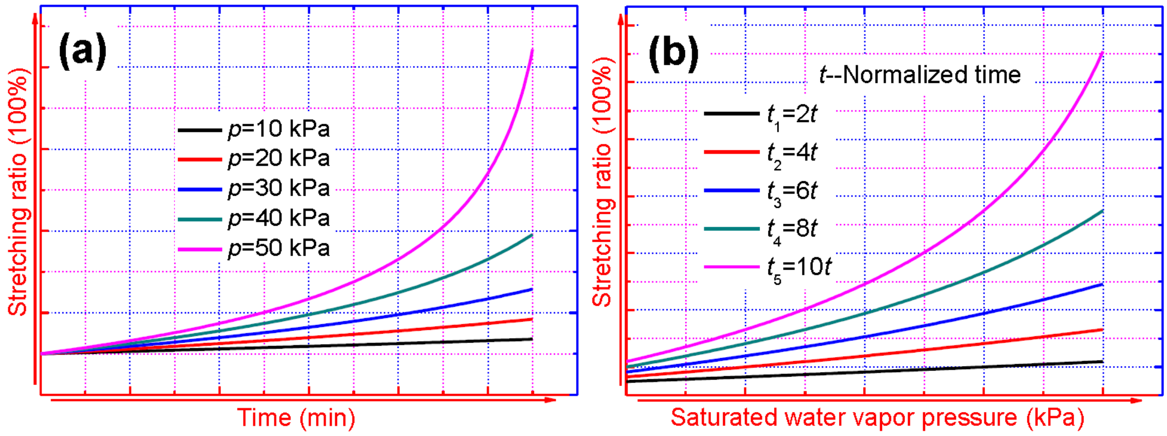

Figure 4 Numerical simulation for the effect of stretching ratio and osmotic pressure on the frequency of PEE-PPy composite in response to water gradient. (a) χ=0.0, 0.2, 0.5, 1.0 and 1.2; (b) t_1=1, 2, 3, 4 and 5t.

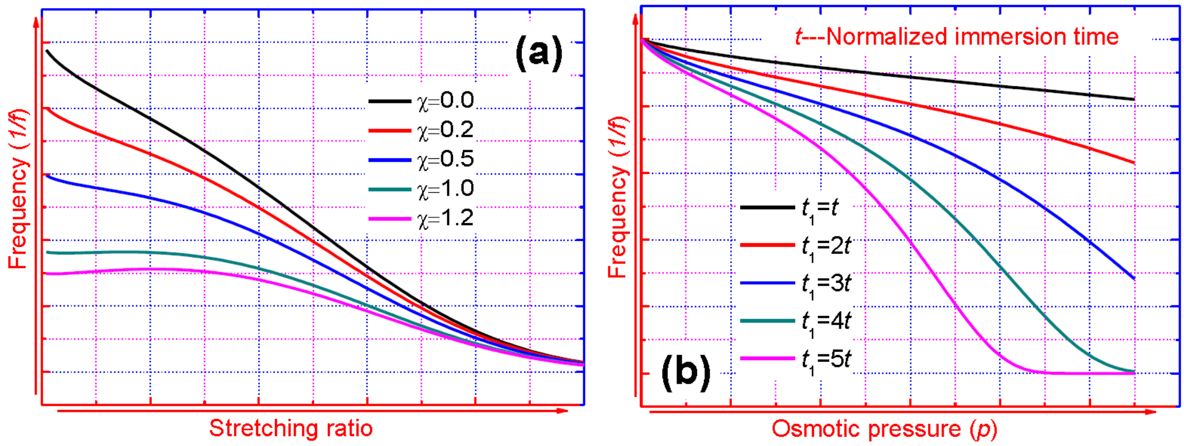

Figure 5 Numerical simulation for the constitutive relation of stress and stretching ratio. (a) χ =0, 0.5, 0.7, 1.0 and 1.2; (b) λ_2/λ_1 =1.25, 1.5, 2.0, 2.5 and 3.0.

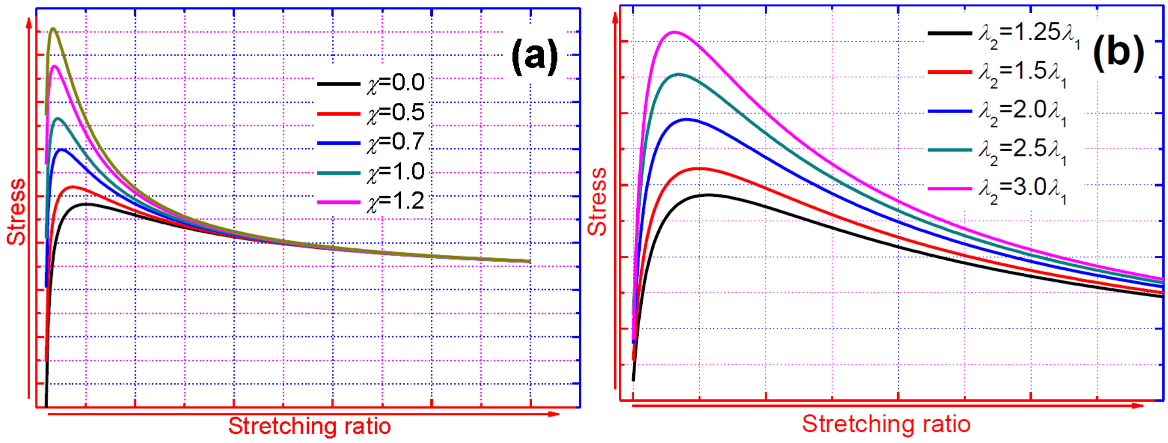

Figure 6 An exponential correlation of the flipping frequency of flipping motion and the saturated water vapour pressure of the PEE-PPy composite [pentaerythritol ethoxylate (PPE) and Polypyrrole (PPy)]. The comparison between the previously experimental data obtained from Ma *et al.*, 2013 and the fitting plots and simulation result of Equation 20.

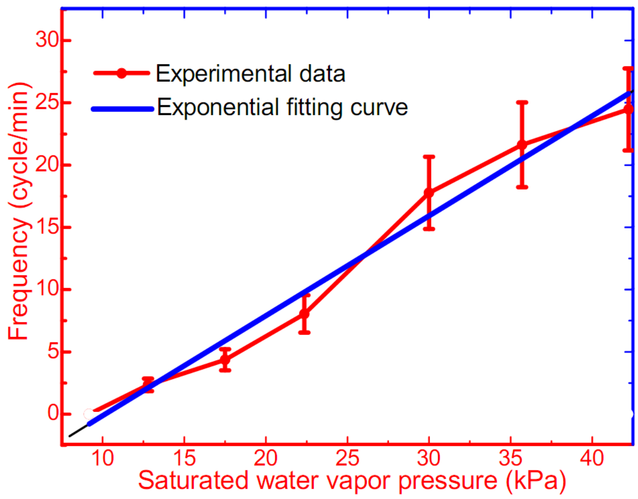

Figure 7 Numerical simulation for the contractile stress in the PEE-PPy composite upon water sorption and desorption. (a) Mechanical performance of the PEE-PPy composite upon water sorption and desorption at a fixed value of λ_2/λ_1; (b) Mechanical performance of the PEE-PPy composite upon water sorption and desorption at λ_2/λ_1=1.25, 2.0 and 3.0.

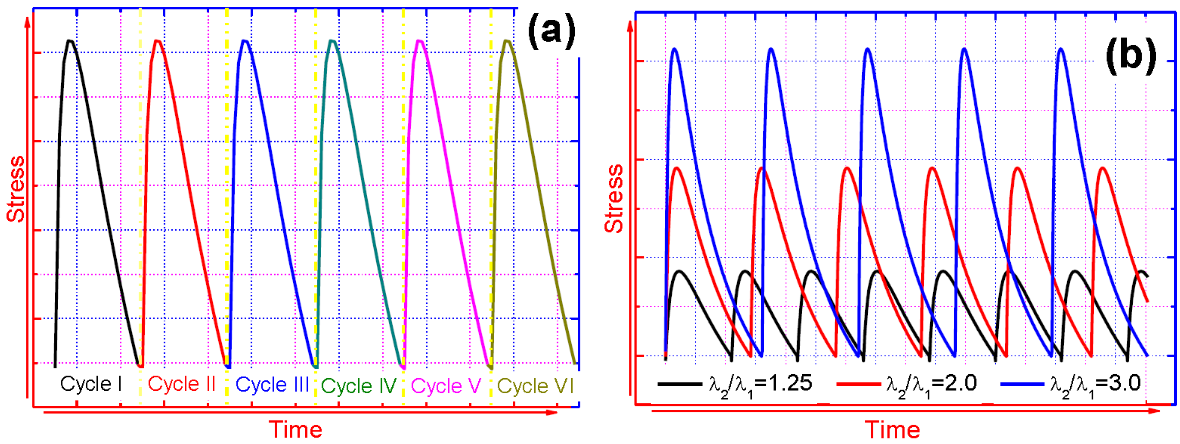

Figure 8 Numerical simulation for the constitutive relationship between flipping frequency and atmospheric pressure for PEE-PPy composite. (a) $pV = 1.0\Delta E$, $0.8\Delta E$, $0.6\Delta E$, $0.4\Delta E$ and $0.2\Delta E$; (b) $\sigma\varepsilon = 1.0\Delta E$, $0.8\Delta E$, $0.6\Delta E$, $0.4\Delta E$ and $0.2\Delta E$.

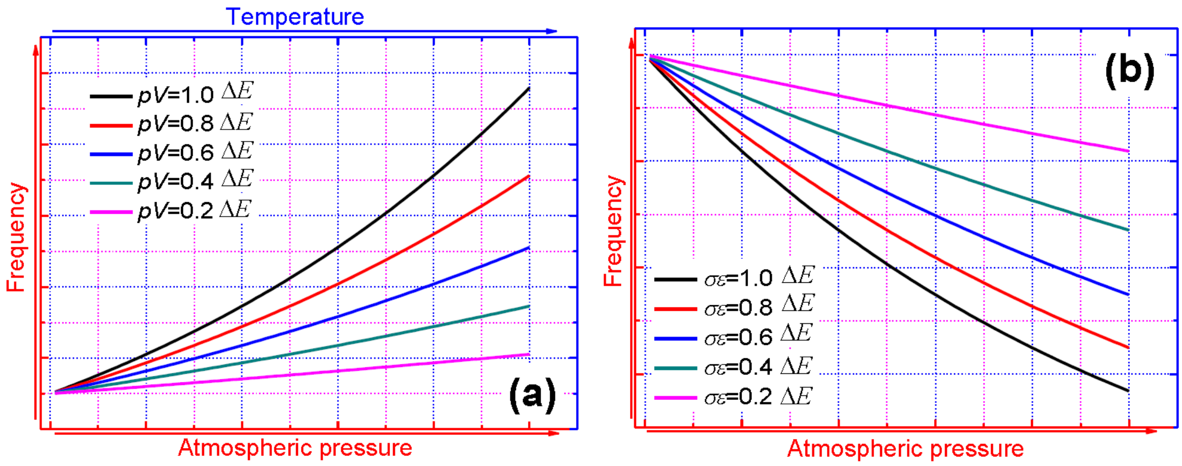

Figure 9 An exponential constitutive relationship of flipping frequency and the cargo of the PEE-PPy composite. The comparison between the previously experimental data obtained from Ma *et al.*, 2013 and the fitting plots and simulation result of Equation 21.